Interactions between heterogeneous cell walls and two procyanidins: Insights from the effects of chemical composition and physical structure

Xuwei Liu, Catherine M.G.C. Renard, Sylvie Bureau, Carine Le Bourvellec

Interactions between heterogeneous cell walls and two procyanidins: Insights from the effects of chemical composition and physical structure

Xuwei Liu[a], Catherine M.G.C. Renard[a,b], Sylvie Bureau[a], Carine Le Bourvellec[a]*

[a]INRAE, Avignon University, UMR408 SQPOV, F-84000 Avignon, France

[b]INRAE, TRANSFORM, F-44000 Nantes, France

Corresponding authors*

Carine Le Bourvellec (carine.le-bourvellec@inrae.fr)

INRAE, UMR408 SQPOV « Sécurité et Qualité des Produits d'Origine Végétale »

228 route de l'Aérodrome

CS 40509

F-84914 Avignon cedex 9

Tél: +33 (0)4 32 72 25 35

Fax: +33 (0)4 32 72 24 92

Others authors

Xuwei Liu: xuwei.liu@inrae.fr

Catherine M.G.C Renard: catherine.renard@inrae.fr

Sylvie Bureau: sylvie.bureau@inrae.fr

19

Graphical Abstract

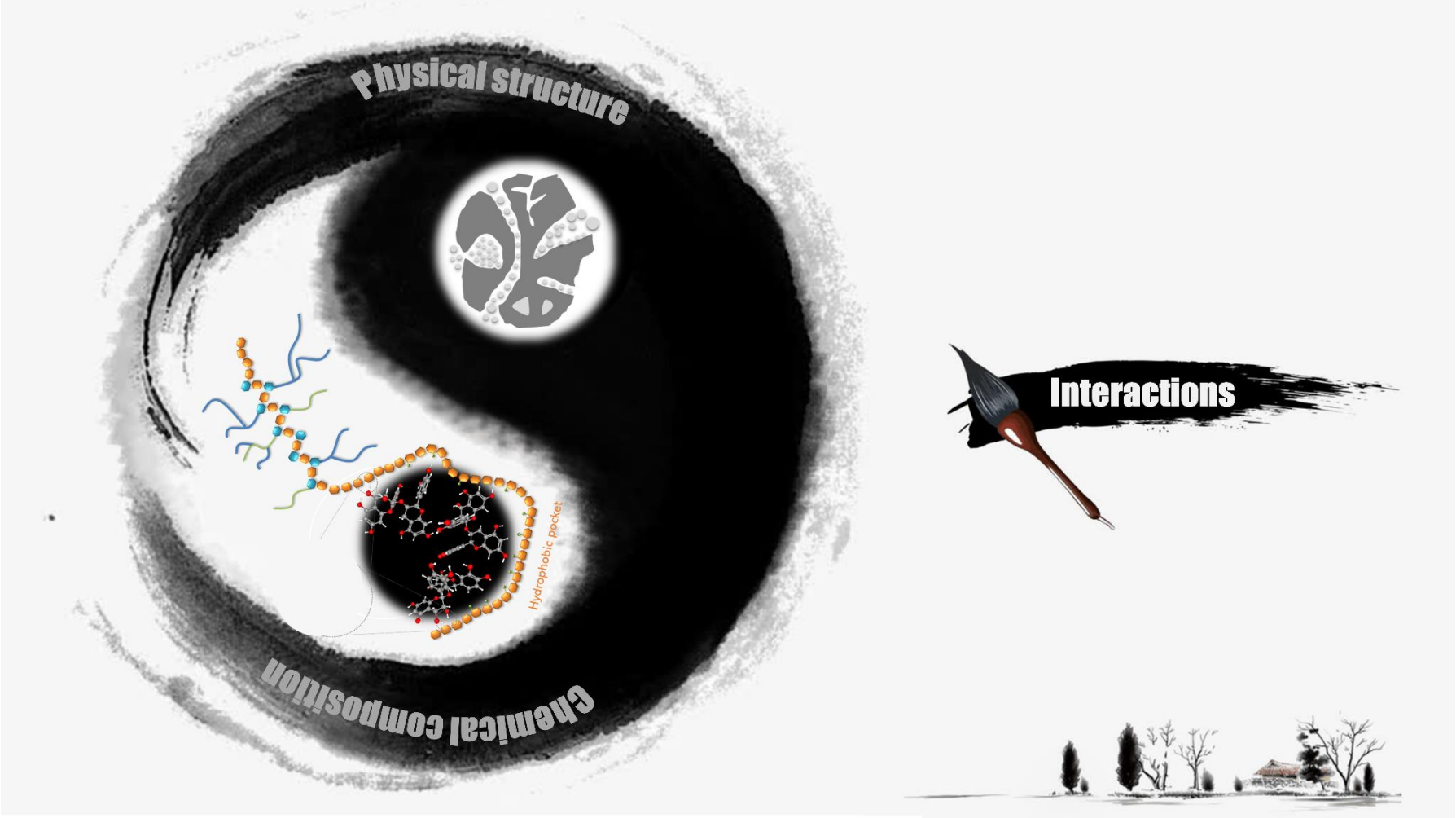

20

Abstract

Cell wall polysaccharides (CWPs) and phenolic substances, e.g., procyanidins, widely co-exist in fruit and vegetables and interact in complex patterns during chewing, food processing and in *vivo* digestion, impacting the food physicochemical and nutritional qualities. Interactions were characterized between two procyanidins and heterogeneous CWPs (four native and twelve modified) from apple, beet and kiwifruit presenting various chemical compositions and physical structures. ATR-FTIR discriminated the complexes from the initial purified procyanidins and CWPs. Langmuir isotherms and ITC indicated that native CWPs, from all botanical origins, had a higher affinity for procyanidins than the modified ones, which were all poorer in pectins. The CWPs that interact more with procyanidins were characterized by their high pectin content and linearity, and high porosity. Increasing the molecular size of procyanidins increased their complexation with CWPs. This work is an important guide to the encapsulation and controlled release of active compounds and the subsequent respective digestive behavior and human health.

Keywords: Polyphenols, Condensed tannins, Polysaccharides, Adsorptions, Porosity, Composition

Abbreviations:

$\overline{DP}n$: number-average degree of polymerization of procyanidins; DM; degree of methylation; AIS, Alcohol Insoluble Solids; ATR-FTIR, Attenuated Total Reflectance Fourier Transform Infrared Spectroscopy; Isothermal Titration Calorimetry, ITC.

1. Introduction

Cell walls and polyphenols are important components of the dietary fiber complexes in plant-based foods. They coexist in plants in a separated cell compartment (Renard, Watrelot, & Le Bourvellec, 2017). The interactions between cell walls and polyphenols may occur during chewing, pre-consumption food processing and subsequent digestion, which modify their structure and composition, thereby affecting their bioefficacy or modulating gut microbiota (Loo, Howell, Chan, Zhang, & Ng, 2020). There seems to be a lack of understanding of the interactions between the different components in the food matrix. This may limit the possibility of linking the specific components to the potential effects of diet, particularly the role of macromolecular polyphenols such as procyanidins. These procyanidins can spontaneously and quickly bind to the cell walls through hydrogen bonding or hydrophobic interaction (Liu, Le Bourvellec, & Renard, 2020; Renard, Baron, Guyot, & Drilleau, 2001; Renard et al., 2017). However, the knowledge of the influence of different types of cell walls (plant origin or processing modification) on the interactions is still lacking.

Plant cell walls are the extracellular matrices surrounding plant cells, which determine the texture of plant-based food (Carpita & Gibeaut, 1993). The dominant thin, hydrophilic and highly hydrated type I cell wall of fruit and vegetables (Waldron, Smith, Parr, Ng, & Parker, 1997) is one of the major source of dietary fiber in human food. It consists of a network of cellulose microfibrils, tethered by hemicelluloses

such as xyloglucans, xylans and mannans, embedded in an amorphous matrix constituted mostly of pectins. These cell walls are very diverse, depending on the composition, size distribution, shape, charge, extractability and combination of their constituent components. They are susceptible to physiochemical transformation reactions during food processing, thereby changing their structure and leading to changes in their functional characteristics. For example, textural alterations related to changes in cell wall porosity impact affinity for procyanidins (Le Bourvellec, Bouchet, & Renard, 2005). In addition, the presence of polyphenols can also change the functional properties of cell wall polysaccharides. For example, feruloylated arabinans can inhibit the softening of radishes during thermal processing (Li, Liu, Tu, Li, & Yan, 2019). The polysaccharide-polyphenol aggregation may decrease the viscosity of a polysaccharide solution (Tudorache & Bordenave, 2019). Therefore, the application of these interactions could improve the development of functional polysaccharides in the food industry.

Polyphenols are broadly distributed in fruit and vegetables, and have a positive effect on human health. Some unesterified phenolic acids and glucosylated monomeric polyphenols are easily absorbed in the upper digestive tract, while macromolecular polyphenols, e.g., procyanidins, are poorly absorbable (Santhakumar, Battino, & Alvarez-Suarez, 2018; Saura-Calixto & Pérez-Jiménez, 2018) and reach the colon. However, many studies have shown that the cell wall-polyphenol complexes can improve the metabolization of polyphenols in the colon (Le Bourvellec et al., 2019; Loo et al., 2020; Phan et al., 2020; Tarko & Duda-Chodak,

2020). Microbiological enzymes in the colon can promote the metabolism of the polyphenols from the complexes, and further bioprocess them from a non-absorbable form to a bioavailable one. Simultaneously, the interactions between polyphenols and cell walls and commensal microorganisms during the digestion process can adjust the balance between the growth of beneficial bacteria and pathogenic microorganisms (Dobson et al., 2019). A comprehensive understanding of the cell wall-macromolecular polyphenol interactions may enable food manufacturers to take full advantage of these beneficial effects.

Cell wall-procyanidin interactions can be mediated by their morphology, chemical composition and molecular architecture, that is, their porosity, the characteristics of their constitutive pectins, such as side-chains and branching ratios, molar mass, degree of esterification, functional groups, and conformation (Liu et al., 2020; Liu, Renard, Rolland-Sabaté, & Le Bourvellec, 2021). Cell walls with high pectin contents have higher affinities for procyanidins, as in the case of pear tissues where the affinity decreases in the order: parenchyma cells > mesocarp (i.e., flesh) hypanthium > stone cells > epidermis (Brahem, Renard, Bureau, Watrelot, & Le Bourvellec, 2019). Cell walls are complex and composed of heterogeneous polymers, of which, pectins have the highest affinity for procyanidins (Le Bourvellec & Renard, 2005; Le Bourvellec, Watrelot, Ginies, Imberty, & Renard, 2012). Moreover, high affinities are typically observed between highly methylated pectins and highly polymerized procyanidins (Watrelot, Le Bourvellec, Imberty, & Renard, 2013). Concerning branching of pectins, the general rule can be summarized as follows: the

more linear the structure and the less branching areas of pectins in the cell walls, the better their association with procyanidins (P. A. R. Fernandes et al., 2020; Liu, Renard, Rolland-Sabaté, & Le Bourvellec, 2021; Watrelot, Le Bourvellec, Imberty, & Renard, 2014). This result also applies to the interaction with anthocyanins (Koh, Xu, & Wicker, 2020). For polyphenols, highly polymeric procyanidins with more hydroxyl and aryl rings bind more tightly to cell walls (Bindon, Smith, & Kennedy, 2010; Renard et al., 2017; Tang, Covington, & Hancock, 2003). However, what happens when these influencing factors are placed in the same cell wall-procyanidin interaction system? Do they act as antagonists or synergists? This still remains to be elucidated.

Although the interactions between the cell walls and procyanidins have been the focus of previous research (Brahem et al., 2019; Le Bourvellec et al., 2005; Le Bourvellec, Guyot, & Renard, 2004; Le Bourvellec & Renard, 2005; Renard et al., 2001), to date, there does not appear to be systematic interaction studies which investigate the impact of botanical origins, processing and maturity modifications and evolutions of cell walls in the establishment of cell wall-procyanidin associations. We are now interested in identifying the cell wall factors, that is, their spread and diversity of structures and composition, that may influence their interactions with procyanidins. In the current work, we examined the capacity of sixteen cell walls, from apple, beet and kiwifruit at two maturity stages (ripe and overripe) differing in both their physical and chemical characteristics to adsorb procyanidins. Interactions were quantified via Langmuir isotherms, as well as isothermal titration calorimetry to

measure thermodynamic changes caused by non-covalent binding. A better understanding of the interactions between plant cell wall polysaccharides and polyphenols (especially procyanidins, important macromolecular antioxidants) is crucial for the development of plant-based food industry.

2. Material and methods

2.1. Standard

Sugar standards (arabinose, mannose, fucose, xylose, rhamnose, and galactose) and phloridzin were purchased from Fluka (Buchs, Switzerland). Methanol-d_3 was from Acros Organics (Geel, Belgium). 4-Coumaric acid was provided from Extra synthese (Lyon, France). All other reagents and solvents were of analytical grade.

2.2. Procyanidins extraction, purification and analysis

Procyanidins of DP12 and DP39 were prepared from apple fruits (*Malus* × *domestica* Borkh.) of the 'Marie Menard' and 'Avrolles' cider cultivars, respectively, as described in Liu, Renard, Rolland-Sabaté, Bureau, & Le Bourvellec (2021). Briefly, this included extraction by aqueous acetone from the freeze-dried apple powders after washing by hexane and methanol, purification on a LiChrospher 100 RP-18 (12 μm, Merck, Darmstadt, Germany) column, concentration and storage under vacuum at -80 °C.

Purified procyanidins were characterized by high-performance liquid chromatography with diode array detection (with/without thioacidolysis) on a

149 Shimadzu Prominence system (Kyoto, Japan) as described in principle by Guyot,
150 Marnet, Sanoner, & Drilleau (2001). The separation condition were as described by
151 Le Bourvellec et al. (2011).

152 **2.3. Preparation and characterization of cell wall polysaccharides**

153 Sixteen cell walls were prepared as described by Liu, Renard, Rolland-Sabaté,
154 Bureau, et al. (2021). In brief, Alcohol-Insoluble Solids (AIS) were first prepared
155 from apple, beet and kiwifruit (ripe and overripe) parenchyma, and named native
156 apple cell wall (ACN), native beet cell wall (BCN), native kiwifruit cell wall ripe
157 (KCRN), native kiwifruit cell wall overripe (KCON). Then the four native cell walls
158 modified by heating in a citrate-phosphate solution (0.1 mol/L) at pH 2.0, 3.5 or 6.0,
159 and the insoluble cell wall residues were retained; the extracted pectins have been
160 used in another study (Liu, Renard, Rolland-Sabaté, & Le Bourvellec, 2021). The
161 modified insoluble cell wall residues were used for the following experiments, i.e.,
162 apple cell walls modified at pH 2.0/3.5/6.0 (named AC2/3/6, respectively), beet cell
163 walls modified at pH 2.0/3.5/6.0 (named BC2/3/6, respectively), kiwifruit cell walls
164 ripe modified at pH 2.0/3.5/6.0 (named KCR2/3/6, respectively) and kiwifruit cell
165 walls overripe modified at pH 2.0/3.5/6.0 (named KCO2/3/6, respectively).

166 Cell wall compositions were analyzed as described by Liu, Renard,
167 Rolland-Sabaté, Bureau, et al. (2021). Approximately 10 mg of cell walls were
168 prehydrolyzed with 72% sulfuric acid (250 µL) for 1 h at room temperature (Saeman,
169 Moore, Mitchell, & Millett, 1954). Neutral sugars were analyzed as alditol acetates

(Englyst, Wiggins, & Cummings, 1982) by GC-FID HP 5890 Series II (Agilent, Inc., Palo Alto, USA). Galacturonic acid was measured by the meta-hydroxyl-diphenyl assay using a spectrophotometer (V-530 Jasco, Tokyo, Japan). The methanol content was measured by stable isotope dilution assay using headspace-GC-MS (QP2010 Shimadzu, Kyoto, Japan) after saponification. The acetic acid content was measured by the acetic acid assay kit (K-ACET, ACS Manual Format, Megazyme International, Ireland). Ferulic acid was released by saponification according to the method of Micard, Renard, & Thibault (1994) by spectrophotometry (V-530Jasco, Tokyo, Japan).

Brunauer-Emmett-Teller (BET) isotherms (Brunauer, Emmett, & Teller, 1938) were used to determine the surface area of the cell walls by nitrogen adsorption isotherms at -196 °C using the Micromeritics AZAP 2010 system and monitored by AZAP 2010 version 5.01 (Micromeritics, Norcross, GA, USA).

The water-binding capacity was measured by filtration method using approximately 250 mg (dry weight) of cell walls left to soak with 10 mL of water containing NaN_3 (1 g/l) for 1 h at room temperature, then filtered and dried (103°C, overnight). The water binding capacity (WBC) was calculated as follows:

$$WBC\ (g/g) = (M2 - M3) / (M3 - M1) \times 100\ \%. \quad \text{(Eq. 1)}$$

With M1: weight of filter, M2 total weight after filtration and M3 after drying. Each sample was analyzed in triplicate.

2.4. Procyanidin-cell wall interactions

2.4.1. Binding isotherm methodology

The experiments were performed (duplicate) at 25 °C using buffer (citrate/phosphate system, pH 3.8, ionic strength 0.1 mol/L) according to Renard et al. (2001). The procyanidin solution (from 0.25 to 12 g/L) and the cell wall suspension (5 mg/mL) were incubated under agitation in 8 mL empty Sep-pack preparation columns. After incubation, the free procyanidins solution and the cell wall-procyanidin complexes were isolated by filtering (20 µm porosity). The free procyanidins content was measured by spectroscopy at 280 nm (JASCO V-730 UV-visible spectrophotometer, Tokyo, Japan). Adsorbed procyanidins were measured by deducting the amount in the supernatant from that in the initial procyanidin solution. The average degree of polymerization of procyanidins ($\overline{DP}n$) was calculated as the molar ratio of all flavan-3-ol units (thioether adduct plus terminal units minus (+)-catechin and (-)-epicatechin naturally present in the samples and determined by analysis of the samples by HPLC-DAD with and without thiolysis) to (+)-catechin and (-)-epicatechin corresponding to the terminal units minus (+)-catechin and (-)-epicatechin naturally present in the samples and determined by analysis of the samples by HPLC-DAD with and without thiolysis.

The binding isotherms were interpreted according to the type-I Langmuir approach (Renard et al., 2001), which expresses bound solute (procyanidins) PP_b (in g/g of adsorbent) as a function of the free solute (procyanidins) concentration [PP_f] at equilibrium.

$$PP_b = \frac{N_{max} K_L [PP_f]}{1 + K_L [PP_f]} \quad \text{(Eq. 2)}$$

where N_{max} is the total amount of available binding sites (expressed in g/g adsorbent) and K_L is an apparent affinity constant (in L/g).

2.4.2. Isothermal Titration Calorimetry (ITC)

The thermodynamic parameters changes caused by the cell wall-procyanidin interactions were measured by ITC using TAM III microcalorimeter (TA instruments, USA) as describe by Liu, Renard, Rolland-Sabaté, & Le Bourvellec (2021). In brief, purified procyanidins (30 mmol/L in (-)-epicatechin equivalent) and cell walls (ca. 8 mg) were dissolved and suspended, respectively, in the same citrate/phosphate buffer pH 3.8, ionic strength 0.1 mol/L. The procyanidin was titrated into the sample cell by 50 injections of 5 µL; each injection lasted 5 s, with separating delay of 900 s for return to horizontal baseline. The content of the sample cell was stirred throughout the experiment at 90 rev/min. Blanks (titration of procyanidin fractions into citrate/phosphate buffer) are deducted from sample titration experiments. Experiments were performed in duplicates. All errors shown in the paper are based on the accuracy of the data fitting.

2.4.3. ATR-FTIR spectra

The cell wall samples retained by filtration after the binding isotherm experiment were further analyzed by ATR-FTIR. Cell wall-procyanidin complexes were selected at four concentrations in binding isotherm experiment, i.e., the initial procyanidin concentrations added were 0.25, 1, 6 and 12 g/l. The ATR-FTIR spectra of cell walls,

procyanidins and freeze-dried complexes were recorded in triplicate (16 scans per spectrum, 4000 to 600 cm^{-1}) using a Tensor 27 FT-IR spectrometer (Brucker Optics, Wissembourg, France) equipped with a single-reflectance horizontal ATR cell (Golden Gate equipped with diamond crystal, Bruker Optics). Spectra were analyzed and controlled by OPUS software Version 5.0 as described by Liu, Renard, Rolland-Sabaté, Bureau, et al. (2021).

2.5. Statistical analysis

Results were expressed as mean values, and their reproducibility presented as the pooled standard deviation (Pooled SD) (Box, Hunter, & Hunter, 1978). MATLAB 7.5 software (Mathworks Inc., Natick, MA, USA) with SAISIR package (Cordella & Bertrand, 2014) was used for pre-processing (baseline correction and standard normal variate) and Principal Component Analysis (PCA). Calculated and observed Langmuir curves were fitted by minimizing the sum of the square of the difference between observed and calculated values to obtain the Langmuir parameters (K_L and N_{max}) using the solver package of Microsoft Excel. Moreover, the confidence intervals ($P > 0.95$) of the Langmuir formula's constants were calculated using the Marquardt estimation method of the non-linear regression package of XLSTAT (version 2020.1.1, Addtionsoft SARL, Paris, France). Heatmap was performed with Python 3.5 software using the Seaborn package (Waskom, 2014).

3. Results

3.1. Composition and structure of the macromolecules and cell wall complexes

3.1.1. Procyanidin fractions

The two apple varieties, i.e., ‘Marie Ménard’ and ‘Avrolles’, were selected to obtain two procyanidins with different degree of polymerization (Le Bourvellec, Guyot, & Renard, 2009). The purified extracts contained about 850 mg/g of phenolic compounds, mainly procyanidins plus traces of other phenolic compounds (Supplementary Table 1). ‘Marie Ménard’ and ‘Avrolles’ procyanidins were composed of more than 99 % (-)-epicatechin units and differed by their degree of polymerization ($\overline{DP}n$ = 12 and 39, respectively). All the results were in accordance with (Le Bourvellec et al., 2012; Liu, Renard, Rolland-Sabaté, & Le Bourvellec, 2021).

3.1.2. Cell wall polysaccharides

Detailed chemical compositions of the cell walls are available in our previous paper (Liu, Renard, Rolland-Sabaté, Bureau, et al., 2021) and the sugar ratios based on the sugar content, specific surface area and water binding capacity for cell walls were calculated (Table 1). A large diversity was obtained on two major parameters, namely (i) the nature and levels of cell wall polymers and (ii) physical characteristics, which further varied independently in this series of cell walls. Concerning the chemical composition and physical structure, apple cell walls were characterized by high xylose content, signaling presence of xylogalacturonans and fucogalactoxyloglucans (Le Bourvellec et al., 2004; Renard, Voragen, Thibault, & Pilnik, 1990, 1991), with intermediate specific surface area and relatively high water-binding capacity. Only beet cell walls contained detectable ferulic acids. They

also had the highest content of pectic neutral sugar side-chains, notably arabinans, and the highest acetyl contents, with a high specific surface area. Kiwifruit cell walls appeared to be the richest in homogalacturonans (conservely, contained pectins with the highest linearity), with the lowest side-chain, arabinose/galactose ratio and acetyl content, with a relatively low specific surface area.

All these characteristics were further modulated after processing at different pH values. For example, at pH 2.0, arabinan or galactan side-chains in the cell walls were lost due to acid hydrolysis, while galacturonic acid and DM were retained to the greatest extent possible. β-elimination reduced the content of galacturonic acid and esterification (DM and Ac.A) in the cell walls after modification at pH 6.0. Pectin depolymerization was least significant and structural modification modest (both acid hydrolysis and β-elimination) at pH 3.5. Different pH modifications enhanced or reduced, to varying degrees, the porosity/specific surface area and water-binding capacity of the cell walls. The ferulic acid cross-linked to the cell wall was present only in the beet cell wall.

Therefore, a large diversity of structural features was obtained in the cell wall set for structure linearity, branching degree and length of side-chains, arabinose/galactose ratio, degree of methylation and acetylation, specific surface area and water-binding capacity. In addition, these factors, which were assigned to the cell wall to influence their interactions, showed varying degrees of importance.

3.2. Global characterization by ATR-FTIR spectroscopy

296 ATR-FTIR can be used to detect changes in the main components of cell wall
297 polysaccharides as well as their modification by other components (Liu, Renard,
298 Bureau, & Bourvellec, 2021). On the principal component analysis, the first two
299 principal components (PC1 48.5 % and PC2 22.7 %) explained 71.2% of the total
300 variance (Fig. 1A). Cell walls, cell wall-procyanidin DP12/39 complexes and
301 procyanidins were separated into three distinct groups. Within the cell
302 wall-procyanidin group, complexes constituted two distinct subgroups: cell wall
303 associated with a low procyanidin concentration (0.25 g/l and 1 g/l) and a high
304 procyanidin concentration (6 g/l and 12 g/l). A gradation of the groups was observed
305 along the PC1 from the left to the right with the increasing of procyanidin
306 concentration.

307 No clear discrimination according to botanical origins, processing conditions or
308 procyanidin sizes was obtained. The loadings on PC1 and PC2 revealed similar
309 patterns and some relevant wavenumbers (Fig. 1B). Along the PC1 axis, the samples
310 were distributed owing to the presence or absence of procyanidins (Fig. 1A). PC1
311 separated cell walls on the left bottom, cell wall-procyanidin complexes in the middle
312 and purified procyanidins on the right bottom according to the presence of linked
313 procyanidins or/and purified cell wall/procyanidin complexes. The negative loadings
314 of PC1 were characterized by the peaks at 1740 and 1015 cm^{-1} which could be due to
315 pectic compounds. Positive loadings for PC1 concerned wavenumbers mostly
316 characteristic of procyanidins (1604, 1519, 1440, 1284 and 1196 cm^{-1}), which
317 progressively increased from 0.25 g/l to 12 g/l. PC2 allowed discrimination between

318 apple/beet cell wall-procyanidin complexes and kiwifruit cell wall-procyanidin
319 complexes in the middle of plot (Fig. 1A).

320 **3.3. Binding isotherms**

321 The binding isotherms of all cell wall-procyanidin complexes (DP12 and DP39)
322 were obtained by placing the suspended cell walls in contact with procyanidin
323 solutions. The isotherms are illustrated by the Langmuir formulations (Eq. (2)) in Fig.
324 2 and the Langmuir parameters (K_L and N_{max}) were calculated (Table 2), both in the
325 form of per g or per m^2 of adsorbent. The data were fitted satisfactorily ($r^2 > 0.85$)
326 using the Langmuir isotherm formula. The amount of adsorbed procyanidins
327 increased with their concentration and finally reached a plateau at high concentrations
328 indicating cell wall saturation (Fig. 2).

329 **3.3.1. Interactions with Procyanidins of DP 12**

330 Isotherm curves varied depending on the composition and the structure of the cell
331 walls (Fig. 2). For the isothermal adsorption curve of procyanidin DP12, beet cell
332 walls had the highest saturation level (plateau of the curve) of bound procyanidins and
333 the highest affinity (slope of the curve) together with apple cell walls. Moreover, after
334 processing, two distinct changes could be noted between chemical compositions and
335 physical surface morphology for different cell walls: ACs, BC2/3 and KCOs cell
336 walls were characterized by a decrease of bound procyanidin after modification. This
337 may be attributed to the loss of pectins from the native cell walls. By contrast, affinity
338 increased for KCOs and BC6, which may be due to an increase of their specific

surface area after processing, thus increasing their adsorption capacity for the procyanidin DP12. The Langmuir constants (K_L and N_{max}) obtained after fitting confirmed these results (Table 2A).

The different chemical compositions and physical surface morphologies observed between botanical origins and after processing had an impact on both apparent affinity (K_L) and apparent saturation level (N_{max}). ACN, BC3, KCRN, KCR6 and KCON/2/3 had close K_L values between 0.21 L/g and 0.29 L/g, while their apparent saturation level (N_{max}) ranged from 0.39 to 0.75 g/g. These could be due to two contrasting observations: (i) either all their features were at an intermediate level, e.g., ACN with moderate pectin linearity (homogalacturonan chains), neutral sugar side-chains and specific surface area; or (ii) they combined features at the two extremes, e.g., KCON had the highest pectin linearity and the lowest specific surface area. BC6 with the highest specific surface area (16.7 m^2/g) had the highest affinity (K_L=0.54 L/g). This may be due to the fact that the morphology of large specific surface area favors the stacking of intermediate-size procyanidins. Conversely, AC2/3/6 and KCR2 had relatively low affinity ($\leq$ 0.17 L/g) and high saturation level ($\geq$ 0.70 g/g), which may be explained by the fact that they had at least two of the following features, namely relatively low pectin linearity, low specific surface area, low degree of methylation or high xylose contents.

The apparent Langmuir parameters were also converted as a function of the amount of procyanidins bound per cell wall surface area (Table 2B). This expression

had most impact on the relative ranking of cell walls which had a larger specific surface area. An increase of cell wall surface area was accompanied by a decrease of K_L and N_{max} related to cell walls with lower surface areas so to their physical characteristics.

Table 2B also provides cell wall-procyanidin interaction characteristics (the amount of bound procyanidins and $\overline{DP}n$ of free procyanidins). The average amount of bound procyanidins varied between 0.061 g/g cell wall (AC6) and 0.091 g/g (BC6), corresponding to 32 % and 53 % of the initial added procyanidins. Different levels of bound procyanidins were found for each cell wall. The binding levels of native cell walls could be ranked: ACN ≈ BCN > KCRN > KCON. For AC2/3/6 and BC2/3, the amount of bound procyanidins decreased after pH modifications, while conversely for BC6, KCR3/6 and KCO2/3/6 it increased. Cell walls with higher specific surface area had a higher affinity for procyanidin DP12. The initial procyanidin fractions were more polymerized ($\overline{DP}n$ = 12) than the free procyanidins remaining in the supernatant (3.7 < $\overline{DP}n$ < 4.5) after interaction. Therefore, all cell walls were selective for highly polymerized procyanidins.

3.3.2. Interactions with Procyanidins of DP 39

The binding isotherms for cell walls and procyanidin DP 39 are presented in Fig. 2. Compared to procyanidin DP 12, the amount of bound procyanidins were higher for the highly polymerized fractions (DP 39). Binding isotherms demonstrated the key role of the $\overline{DP}n$ in modulating the interactions between cell walls and procyanidins.

381 The calculated apparent constants are given in Table 2. For ACs, BCN/2/3, and KCO3,
382 higher apparent affinities (K_L) were obtained when $\overline{DP}n$ increased. However, for
383 BC6, KCRs and KCON/2/6, lower apparent affinities (K_L) were obtained when $\overline{DP}n$
384 increased. In these cell walls, high content of neutral sugar side-chains, both low
385 degree of methylation and specific surface area may limit their affinity. Their
386 apparent saturation levels (N_{max}) were higher than those of procyanidins of low $\overline{DP}n$
387 (Table 2). These binding isotherms did not reach a stable plateau (Fig. 2), probably
388 due to a lack of data in the high concentration range, i.e., above the limit of
389 procyanidin solubility.

390 The average amount of bound procyanidins varied between 0.084 g/g cell wall
391 (KCR2) and 0.148 g/g (ACN), corresponding to 46 % and 61 % of the initial used
392 procyanidins (Table 2B). The binding levels of native cell walls decreased in the
393 following order: ACN > BCN > KCON > KCRN. For AC2/3/6, BC2/3/6 and KCR2,
394 the amount of bound procyanidins decreased after pH modifications, while it
395 increased for KCR3/6 and KCO2/3/6. The initial procyanidin fractions were more
396 polymerized ($\overline{DP}n$ = 39) than the free procyanidins remaining in the supernatant
397 (12.4 < $\overline{DP}n$ < 21.9). This again indicated that all cell walls were selective for highly
398 polymerized procyanidins.

399 **3.4. Isothermal titration calorimetry**

400 **3.4.1. Interactions with Procyanidins of DP12**

401 Thermodynamic parameters from ITC titration of cell walls by procyanidins

DP12 are shown in Table 3. Typical thermograms were obtained for all cell walls (ca. 8 mg) titrated by procyanidin DP12 (30 mmol/L epicatechin equivalent) with strong exothermic peaks (data not shown). Stoichiometry (defined as ratio of epicatechin/galacturonic acid) was fixed at 0.1 for all cell walls (1 molecule of epicatechin bound 10 units of galacturonic acid) using a one-site model. This value was determine from previous studies (Brahem et al., 2019).

The association constant ranged between 1.0×10^2 M^{-1} and 3.2×10^3 M^{-1} and the top three highest affinities decreased in the following order: ACN > KCRN > KCON (Table 3). ACN with a low (Ara+Gal)/Rha ratio (9.5), both medium Gal A/(Rha+Ara+Gal) ratio (1.2) and specific surface area (5.4 m^2/g), and a high DM (82 %) (Table 1) had the highest affinity for procyanidin DP12, showing that a combination of positive factors contributed to its high interactions. Similarly, KCRN and KCON had a high pectin linearity (homogalacturonan chains) and a low degree of branching, and they also contained a high affinity component, i.e., kiwifruit pectins as shown by Liu, Renard, Rolland-Sabaté, Bureau, et al. (2021). For ACN/2/6, BC6, KCRN and KCON/6, analysis of the thermodynamic contributions ($\Delta G = \Delta H - T\Delta S$) related to the exothermic reactions indicated a strong entropy contribution ($-T\Delta S$ from -18 to -9 kJ/mol) showing that the interactions were mostly driven by entropy. This indicated that the binding system was mostly driven by hydrophobic interactions. By contrast, the enthalpy contributions were high for AC3, BCN/2/3, KCR2/3/6 and KCO2/3 (ΔH from -46 to -12 kJ/mol) indicating that the interactions were mostly driven by hydrogen bonds.

3.4.2. Interactions with procyanidins of DP 39

Titration of all cell walls by procyanidins DP39 showed complex curves characterized by strong exothermic peaks. Thermodynamic parameters are shown in Table 3. To avoid over-fitting, the stoichiometry (n) was also fixed at 0.1 for all cell walls to allow fit and determination of association parameters.

The association constant K_a between cell walls and procyanidins DP39 ranged from 1.0×10^2 M^{-1} to 1.6×10^3 M^{-1} in the decreasing order: KCO2/6 > KCR6 > ACN > AC3 > KCR2 ≈ AC2 > KCRN/3 ≈ KCON/3 > AC6 ≈ BCN/2/3/6. The affinity of the beet cell walls was generally low. Regarding the interactions between all cell walls and procyanidins DP39, contribution of enthalpy (ΔH from -4 to -26 kJ/mol) related to the exothermic reactions indicated that the interactions were mostly driven by hydrogen bonds due to the high number of hydroxyl groups in procyanidins DP39.

4. Discussion

4.1. Comparison of spectroscopy, calorimetry and binding isotherm methods

Using ATR-FTIR, isothermal titration calorimetry and binding isotherm, cell walls with different levels of porosity, pectin linearity (homogalacturonan chains), side-chain abundance, and degree of esterification were shown to interact with procyanidins (DP12 and DP39). The spectra of procyanidins DP12 and DP39 were close, as well as for other procyanidin fractions, e.g., pear procyanidins (Brahem et al., 2019). Therefore, the following characteristic spectra can be used to distinguish between initial cell walls and cell wall-procyanidin complexes. Bands at 1604, 1519

and 1440 cm^{-1} can be attributed to C=C and C-C stretching bond vibrations in typical aromatic rings (Alfaro-Viquez, Esquivel-Alvarado, Madrigal-Carballo, Krueger, & Reed, 2020; Edelmann, Diewok, Schuster, & Lendl, 2001). Bands at 1284 and 1196 cm^{-1} can be assigned to phenolic OH and C-O group deformation vibrations and bending vibrations (Velasco et al., 2014).

Binding isotherms of cell wall-procyanidin interactions were well described by previous research as type I isotherms (the so-called Langmuir isotherms), e.g., apple, pear and grape cell walls (Bindon, Bacic, & Kennedy, 2012; Brahem et al., 2019; Le Bourvellec et al., 2004; Le Bourvellec & Renard, 2005; Renard et al., 2001). However, this fit is an empirical description and is not equivalent to the same mechanism described by Langmuir (Langmuir, 1918) for the adsorption of gases on solid surfaces. This method can provide some adsorption parameters and behaviors. The amount of procyanidins (DP12 and 39) bound to each cell wall ranged from 61 mg/g cell wall to 148 mg/g cell wall, with an apparent affinity constant range of 0.11 to 0.60 L/g. Their interactions detected by ITC seem to be exothermic, and driven by both entropy and enthalpy contributions, which are caused by hydrophobic interactions (or changes in solvation and conformation) and hydrogen bonds, respectively (Leavitt & Freire, 2001; Liu et al., 2020; Poncet-Legrand, Gautier, Cheynier, & Imberty, 2007). The order of magnitudes of their affinity constant (K_a) ranged from 10^2 to 10^3 M^{-1}. These three methods are complementary: (i) rapid and sensitive to detect the presence of procyanidins in complexes (ATR-FTIR); (ii) allowing determination of the binding parameters, e.g., bound amount, K_L and N_{max} (binding isotherms); (iii) enabling

467 access to thermodynamic (enthalpy/enthalpy) changes, i.e., mechanism, and
468 K_a/affinity (ITC).

469 The above indicators are the main evaluation parameters indicating the strength
470 of the interactions. The effect of different cell wall composition/structure on the
471 interactions was assessed by PCA and correlation analysis. The PCA results are
472 presented in Supplementary Fig. 1. PC1 and PC2 explained 52% of the total variance
473 of cell wall characteristics and their interaction with procyanidin DP12 and DP39.
474 According to Supplementary Fig. 1, some interaction parameters were distributed
475 separately for different procyanidins, implying that the mechanisms of interaction
476 may be different. This was also reflected in the correlation analysis (Fig. 3). To be
477 specific, the linearity of pectin was correlated with K_a (by ITC) for procyanidin DP12
478 and 39. This suggested a significant contribution of homogalacturonan content to the
479 affinity. In addition, porosity/surface area (by BET) showed correlation with bound
480 procyanidin DP12 and their K_L (DP12, binding isotherms) and moderate correlation
481 with bound procyanidin DP39 and their K_L (DP39, binding isotherms). This inferred
482 that low polymerized procyanidins are more readily bound by porous cell walls,
483 whereas high polymerized procyanidins may be restricted. Although side-chain
484 abundance and ferulic acid content showed some correlation with K_L, these factors are
485 detrimental to the interactions. This implied that porosity was probably antagonistic to
486 side-chain abundance and ferulic acid content, but that porosity played a dominant
487 role in cell wall-procyanidin interactions.

488 **4.2. Pectin content and linearity in cell walls**

489 Firstly, during heat treatment at different pH, cell walls are modified so that a
490 portion of the soluble polysaccharides are extracted giving extractable pectins. The
491 second point to note is that irrespective of the pectin content of the cell wall starting
492 material, the main goal of our study was to determine the effect of the chemical
493 composition and physical structure of the cell wall on their binding properties for
494 procyanidins. This is because the changes in cell wall adsorption of procyanidins
495 resulting from pectin extraction are already reflected in cell wall modifications. That
496 is, not only the composition changes, but also the porosity of the cell wall increases
497 (i.e., enables more internal cavities) or decreases (i.e., cell wall collapse or shrinkage)
498 with the difference in the original structure or the treatment conditions.

499 The higher affinities for procyanidins DP12/39 were obtained for mostly
500 unmodified cell walls, with both higher K_a and more bound procyanidins. In contrary,
501 lower affinities were observed for most modified cell walls. This confirms the
502 findings of Ruiz-Garcia et al. (2014) who suggested that the removal of pectin
503 significantly reduces the adsorption of proanthocyanidins by cell wall residues,
504 however, despite pectin elimination the cell wall still have and affinity for
505 procyanidins (Le Bourvellec et al., 2012). Native cell walls (A/B/KC/KOCN)
506 exhibited the highest extractable pectin contents, while the modified cell walls, to
507 varying degrees, lost extractable pectins (loss ratio pH 6.0 > 3.5 > 2.0). Extractable
508 pectins have a high binding capacity and affinity for procyanidins (Le Bourvellec et

al., 2005, 2012; Liu et al., 2020; Ruiz-Garcia et al., 2014). Pectin content and linearity did not make a significant difference to the binding capacity, i.e., K_L obtained using binding isotherms, of different cell walls with procyanidins, as other factors are also involved in the regulation of their interactions. The affinity K_a (obtained using ITC) of beet cell walls was relatively lower than that of apple and kiwifruit cell walls. This may be due to their complex arabinan side-chain structures and the presence of ferulic acid covalently linked to arabinans that limit interactions (P. A. R. Fernandes et al., 2020; Liu, Renard, Rolland-Sabaté, & Le Bourvellec, 2021; Watrelot et al., 2014). Binding isotherms appear to be more sensitive than ITC to factors influencing interactions, as they could take into account the physical aspects of the binding.

Different conditions of processing or treatments can also significantly influence interactions. For example, pH 2.0 modification caused removal of most of the neutral sugar side-chains while degrees of methylation remained high, thus increasing the linearity of pectin and homogalacturonan content with high DM in the A/B/KC/KOC2 cell walls. This structure probably caused AC2 and BC2 to bind more procyanidins by stacking than after the other pH treatments, obtained by binding isotherms. However, this trend was not evident for the affinity K_a results obtained by ITC. For kiwifruit cell walls, no relevant pattern was found, probably due to the fact that pH modification did not drastically affect the linearity of pectins insofar as the initial kiwifruit pectins are already linear with low side-chain content, and the other physical factors (e.g., porosity) could also combine to influence this result (Liu et al., 2020).

4.3. Surface area/porosity

BC6, with the lowest pectin linearity and DM, and the highest side-chains and branching ratios, could be expected to have the lowest binding capacity and affinity to procyanidins. This was not the case, however, as it had a relatively high binding capacity and affinity for the procyanidin DP12. This may be attributed to the fact that BC6 had the highest specific surface area (16.7 m^2/g), i.e., the highest porosity, of all cell walls. Solvent exchange drying increased the porosity of the cell walls, which could allow encapsulation of the procyanidins in a more open conformation (Le Bourvellec et al., 2012). The remodeling and loosening of the grape cell wall due to ripening also increased the porosity of cell walls, leading to an increase in the adsorption of proanthocyanidins (Bindon et al., 2012). The porosity of cell walls of different tissues also varies considerably, for example, the stone cells of pears are secondary cell walls with a dense structure and less porosity, and therefore have a lower affinity for procyanidins (Brahem et al., 2019).

Despite the high porosity of BC6, its binding capacity and affinity for procyanidin DP39 was not better than that for DP12. This could be attributed not only to its high branching ratio preventing the entry of larger molecules of procyanidin DP39, but also to the size and type of pore. In general, the limiting pore size of the cell wall is about 5 nm (equivalent to the size of DP34) (Carpita, Sabularse, Montezinos, & Delmer, 1979), while the pores may have slits, interstices, spherical, cylindrical, and conical forms (Liu et al., 2020). These two factors may conjointly modulate the interaction between cell walls with different porosity and procyanidins

552 with different sizes. The water-binding capacity of the cell walls, regulated by
553 porosity levels and cell wall components (Klaassen & Trindade, 2020; Paudel, Boom,
554 van Haaren, Siccama, & van der Sman, 2016), may influence their capacity to adsorb
555 procyanidins, but no causal link can be established between the two at this point.
556 Notedly, the specific surface areas given here are measured as dry matter and may
557 differ in aqueous media, thus the next important work should be to focus on the wet
558 porosity.

559 **4.4. Substitution of the galacturonic acids**

560 Highly methylated pectin has already been demonstrated to have a high affinity
561 with highly polymerized procyanidins (Liu et al., 2020; Watrelot et al., 2013).
562 However, this result may be counterbalanced by other factors in the cell wall. The cell
563 walls modified at pH 6.0, i.e., AC/BC/KCR/KCO6, had the lowest pectin DM in each
564 species due to β-elimination. The binding capacity and affinity of these cell walls for
565 procyanidins were not always the least (Tables 2 and 3). Other cell wall components,
566 e.g., cellulose and hemicelluloses, as well as their physical characteristic like porosity,
567 may combine to influence the final interactions.

568 Beet cell walls had the highest acetic acid content, but it appears not to be a
569 positive factor for interactions. This may be related to a reduction in potential binding
570 sites. Likewise, anthocyanins bind more to low-esterified beet and citrus pectins than
571 to highly esterified pectins (A. Fernandes et al., 2020; Larsen, Buerschaper, Schieber,
572 & Weber, 2019). The reduction in acetic acid increased the number of hydroxyl
573 groups available on the surface, while alleviating the hindrance of groups at adjacent

574 positions on the binding surface, therefore potentially facilitating the accumulation of
575 procyanidins on the cell wall surface.

576 **4.5. Degree of polymerization of procyanidins**

577 Generally, the higher the degree of polymerization of procyanidins, the stronger
578 the interaction with cell walls. For example, the cell walls have higher binding
579 capacities and affinities for the procyanidin DP39 than for DP12 (Table 2). This may
580 be due to the higher number of hydroxyl groups and aryl rings, allowing a higher
581 number of hydrogen bonds and hydrophobic interaction sites. However, there were
582 two trends in the affinity of cell walls for procyanidin DP39. AC3, BCN, KCR2/6 and
583 KCO2 had a higher affinity for DP39 than DP12 by ITC, but ACN/2/6, BC2/3/6,
584 KCRN/3 and KCON/3/6 had a lower affinity for DP39 than DP12 by ITC. It is likely
585 that both porosity and chemical composition were responsible for this result. As
586 discussed in the previous section on porosity, cell walls such as KCR/ON (ca. 1 m^2/g)
587 had a very low porosity and larger procyanidins might not easily enter inside their
588 internal pores. On the other hand, BC2/3/6 had high neutral sugar side-chain
589 branching ratio, together with high ferulic acid content (Table 1). Therefore, this
590 structure might cross-link the side-chains and hindered the available binding sites
591 limiting their interaction with procyanidin DP39. Moreover, the change in
592 entropy/enthalpy also explains this result, as only hydrogen bonding drives the
593 interaction with procyanidin DP39, while both hydrophobic interactions and hydrogen
594 bonds for DP12.

595 Notably, the natural cell wall architecture and organization are also a very

596 important factor, i.e., cell wall matrix interactions (Varner & Lin, 1989). For example,
597 natural pectins can also strongly interact with other cell wall components, such as
598 cellulose, which may limit their potential for interactions with other biomolecules
599 (Broxterman & Schols, 2018). Similarly, the presence of many other covalent or
600 non-covalent interactions such as interactions between cellulose, xyloglucan/xylan
601 and RG-I side-chains, may also limit the exposure of binding sites (Ralet et al., 2016;
602 Zykwinska, Ralet, Garnier, & Thibault, 2005). However, the extent to which these
603 interactions may vary in different plant cell walls may also be an important factor in
604 their interaction with polyphenols. Therefore, future work will require a more precise
605 identification of the architecture and conformation of the cell wall.

606 **5. Conclusions**

607 Cell walls from apple, beet and kiwifruit have different levels of binding
608 selectivity depending on their chemical composition and physical structure. For
609 extractable polysaccharides (soluble state), e.g., pectins, the linearity and degree of
610 methylation were important, but for native and modified cell walls (insoluble state),
611 porosity appears to be a major factor. Binding isotherms play an essential role in the
612 study of physical adsorption. The ranking of factors affecting cell wall selectivity
613 were, for those which favor interactions, high porosity (including the size and type)
614 and pectin linearity and homogalacturonan content (as synergists), while high xylose,
615 ferulic acid and acetic acid contents, and pectin branching were detrimental (as
616 antagonists). Further work is needed to confirm the role of wet porosity (i.e., in
617 suspension) of cell walls.

618 The cell wall structure is generally altered during food processing and digestion.
619 Each cell wall has its own unique chemical composition, molecular architecture and
620 physical structure, and has common and specific responses to processing and
621 digestion. All these factors interact with each other to impact the interactions.
622 Understanding the relations between the chemical and physical factors remains a huge
623 challenge, and more work is needed to clarify the mechanisms involved and internal
624 relationships. Systematic studies of interactions between biomacromolecules allows to
625 better establish a bridge between food processing and the binding/retention of
626 bioactive substances in food industry.

627 **Acknowledgements**

628 LIU Xuwei would like to acknowledge China Scholarship Council (CSC) and Institut
629 National de Recherche pour l'Agriculture, l'Alimentation, et l'Environnement
630 (INRAE) for financial support to his PhD study.

631 **Conflicts of interest**

632 The authors declare no conflicts of interest.

633 **CRediT authorship contribution statement**

634 **Xuwei Liu**: Investigation, Formal analysis, Data curation, Writing - original draft.
635 **Catherine M. G. C. Renard**: Conceptualization, Supervision, Funding acquisition,
636 Project administration, Validation, Writing - review & editing. **Sylvie Bureau**:
637 Investigation, Software, Supervision, Writing - review & editing. **Carine Le**
638 **Bourvellec**: Conceptualization, Supervision, Funding acquisition, Project

administration, Validation, Writing - review & editing.

References

Alfaro-Viquez, E., Esquivel-Alvarado, D., Madrigal-Carballo, S., Krueger, C. G., & Reed, J. D. (2020). Antimicrobial proanthocyanidin-chitosan composite nanoparticles loaded with gentamicin. *International Journal of Biological Macromolecules*, *162*, 1500–1508. https://doi.org/10.1016/j.ijbiomac.2020.07.213

Bindon, K. A., Bacic, A., & Kennedy, J. A. (2012). Tissue-specific and developmental modifications of grape cell walls influence the adsorption of proanthocyanidins. *Journal of Agricultural and Food Chemistry*, *60*(36), 9249–9260. https://doi.org/10.1021/jf301552t

Bindon, K. A., Smith, P. A., & Kennedy, J. A. (2010). Interaction between grape-derived proanthocyanidins and cell wall material. 1. effect on proanthocyanidin composition and molecular mass. *Journal of Agricultural and Food Chemistry*, *58*(4), 2520–2528. https://doi.org/10.1021/jf9037453

Box, G. E., Hunter, W. G., & Hunter, J. S. (1978). *Statistics for Experimenters, an Introduction to Design, Data Analysis and Model Building*. *New-York, Wiley and Sons*.

Brahem, M., Renard, C. M. G. C., Bureau, S., Watrelot, A. A., & Le Bourvellec, C. (2019). Pear ripeness and tissue type impact procyanidin-cell wall interactions. *Food Chemistry*, *275*, 754–762. https://doi.org/10.1016/j.foodchem.2018.09.156

Broxterman, S. E., & Schols, H. A. (2018). Interactions between pectin and cellulose in primary plant cell walls. *Carbohydrate Polymers*, *192*, 263–272. https://doi.org/10.1016/j.carbpol.2018.03.070

Brunauer, S., Emmett, P. H., & Teller, E. (1938). Adsorption of Gases in Multimolecular Layers. *J. Am. Chem. Soc.*, *60*(2), 309–319. https://doi.org/10.1021/ja01269a023

Carpita, N., & Gibeaut, D. M. (1993). Structural models of primary cell walls in flowering plants: Consistency of molecular structure with the physical properties

669 of the walls during growth. *Plant Journal*, *3*(1), 1–30.
670 https://doi.org/10.1111/j.1365-313X.1993.tb00007.x
671 Carpita, N., Sabularse, D., Montezinos, D., & Delmer, D. P. (1979). Determination of
672 the pore size of cell walls of living plant cells. *Science*, *205*(4411), 1144–1147.
673 https://doi.org/10.1126/science.205.4411.1144
674 Cordella, C. B. Y., & Bertrand, D. (2014). SAISIR: A new general chemometric
675 toolbox. *TrAC - Trends in Analytical Chemistry*, *54*, 75–82.
676 https://doi.org/10.1016/j.trac.2013.10.009
677 Dobson, C. C., Mottawea, W., Rodrigue, A., Buzati Pereira, B. L., Hammami, R.,
678 Power, K. A., & Bordenave, N. (2019). Impact of molecular interactions with
679 phenolic compounds on food polysaccharides functionality. In L. B. Isabel C.F.R.
680 Ferreira (Ed.), *Advances in Food and Nutrition Research* (Vol. 90, pp. 135–181).
681 Elsevier Inc. https://doi.org/10.1016/bs.afnr.2019.02.010
682 Edelmann, A., Diewok, J., Schuster, K. C., & Lendl, B. (2001). Rapid method for the
683 discrimination of red wine cultivars based on mid-infrared spectroscopy of
684 phenolic wine extracts. *Journal of Agricultural and Food Chemistry*, *49*(3),
685 1139–1145. https://doi.org/10.1021/jf001196p
686 Englyst, H., Wiggins, H. S., & Cummings, J. H. (1982). Determination of the
687 non-starch polysaccharides in plant foods by gas-liquid chromatography of
688 constituent sugars as alditol acetates. *The Analyst*, *107*(1272), 307–318.
689 https://doi.org/10.1039/an9820700307
690 Fernandes, A., Oliveira, J., Fonseca, F., Ferreira-da-silva, F., Vincken, J., & Freitas, V.
691 De. (2020). Molecular binding between anthocyanins and pectic polysaccharides
692 – Unveiling the role of pectic polysaccharides structure. *Food Hydrocolloids*,
693 105–625. https://doi.org/10.1016/j.foodhyd.2019.105625
694 Fernandes, P. A. R., Le Bourvellec, C., Renard, C. M. G. C., Wessel, D. F., Cardoso,
695 S. M., & Coimbra, M. A. (2020). Interactions of arabinan-rich pectic
696 polysaccharides with polyphenols. *Carbohydrate Polymers*, *230*, 115–644.
697 https://doi.org/10.1016/j.carbpol.2019.115644

Guyot, S., Marnet, N., Sanoner, P., & Drilleau, J.-F. (2001). Direct thiolysis on crude apple materials for high-performance liquid chromatography characterization and quantification of polyphenols in cider apple tissues and juices. In L. Packer (Ed.), *Methods in Enzymology* (pp. 57–70). Elsevier Inc. https://doi.org/10.1016/S0076-6879(01)35231-X

Klaassen, M. T., & Trindade, L. M. (2020). RG-I galactan side-chains are involved in the regulation of the water-binding capacity of potato cell walls. *Carbohydrate Polymers*, *227*, 115353. https://doi.org/10.1016/j.carbpol.2019.115353

Koh, J., Xu, Z., & Wicker, L. (2020). Binding kinetics of blueberry pectin-anthocyanins and stabilization by non-covalent interactions. *Food Hydrocolloids*, *99*, 105–354. https://doi.org/10.1016/j.foodhyd.2019.105354

Langmuir, I. (1918). The adsorption of gases on plane surfaces of glass, mica and platinum. *Journal of the American Chemical Society*, *40*(9), 1361–1403. https://doi.org/10.1021/ja02242a004

Larsen, L. R., Buerschaper, J., Schieber, A., & Weber, F. (2019). Interactions of anthocyanins with pectin and pectin fragments in model solutions. *Journal of Agricultural and Food Chemistry*, *67*, 9344–9353. https://doi.org/10.1021/acs.jafc.9b03108

Le Bourvellec, C., Boas, P. B. V., Lepercq, P., Comtet-Marre, S., Auffret, P., Ruiz, P., … Mosoni, P. (2019). Procyanidin—cell wall interactions within apple matrices decrease the metabolization of procyanidins by the human gut microbiota and the anti-inflammatory effect of the resulting microbial metabolome in vitro. *Nutrients*, *11*(3), 664. https://doi.org/10.3390/nu11030664

Le Bourvellec, C., Bouchet, B., & Renard, C. M. G. C. (2005). Non-covalent interaction between procyanidins and apple cell wall material. Part III: Study on model polysaccharides. *Biochimica et Biophysica Acta - General Subjects*, *1725*(1), 10–18. https://doi.org/10.1016/j.bbagen.2005.06.004

Le Bourvellec, C., Bouzerzour, K., Ginies, C., Regis, S., Plé, Y., & Renard, C. M. G. C. (2011). Phenolic and polysaccharidic composition of applesauce is close to

727 that of apple flesh. *Journal of Food Composition and Analysis*, *24*(4–5), 537–547.
728 https://doi.org/10.1016/j.jfca.2010.12.012
729 Le Bourvellec, C., Guyot, S., & Renard, C. M. G. C. (2004). Non-covalent interaction
730 between procyanidins and apple cell wall material: Part I. Effect of some
731 environmental parameters. *Biochimica et Biophysica Acta - General Subjects*,
732 *1672*(3), 192–202. https://doi.org/10.1016/j.bbagen.2004.04.001
733 Le Bourvellec, C., Guyot, S., & Renard, C. M. G. C. (2009). Interactions between
734 apple (Malus x domestica Borkh.) polyphenols and cell walls modulate the
735 extractability of polysaccharides. *Carbohydrate Polymers*, *75*(2), 251–261.
736 https://doi.org/10.1016/j.carbpol.2008.07.010
737 Le Bourvellec, C., & Renard, C. M. G. C. (2005). Non-covalent interaction between
738 procyanidins and apple cell wall material. Part II: Quantification and impact of
739 cell wall drying. *Biochimica et Biophysica Acta - General Subjects*, *1725*(1), 1–9.
740 https://doi.org/10.1016/j.bbagen.2005.06.003
741 Le Bourvellec, C., Watrelot, A. A., Ginies, C., Imberty, A., & Renard, C. M. G. C.
742 (2012). Impact of processing on the noncovalent interactions between
743 procyanidin and apple cell wall. *Journal of Agricultural and Food Chemistry*,
744 *60*(37), 9484–9494. https://doi.org/10.1021/jf3015975
745 Leavitt, S., & Freire, E. (2001). Direct measurement of protein binding energetics by
746 isothermal titration calorimetry. *Current Opinion in Structural Biology*, *11*(5),
747 560–566. https://doi.org/10.1016/S0959-440X(00)00248-7
748 Li, X., Liu, G., Tu, Y., Li, J., & Yan, S. (2019). Ferulic acid pretreatment alleviates
749 the decrease in hardness of cooked Chinese radish (Raphanus sativus L. var.
750 longipinnatus Bailey). *Food Chemistry*, *278*, 502–508.
751 https://doi.org/10.1016/j.foodchem.2018.10.086
752 Liu, X., Le Bourvellec, C., & Renard, C. M. G. C. (2020). Interactions between cell
753 wall polysaccharides and polyphenols: Effect of molecular internal structure.
754 *Comprehensive Reviews in Food Science and Food Safety*, *19*(6), 3574–3617.
755 https://doi.org/10.1111/1541-4337.12632

Liu, X., Renard, C. M. G. C., Bureau, S., & Bourvellec, C. Le. (2021). Revisiting the contribution of ATR-FTIR spectroscopy to characterize plant cell wall polysaccharides. *Carbohydrate Polymers*, 117935. https://doi.org/10.1016/j.carbpol.2021.117935

Liu, X., Renard, C. M. G. C., Rolland-Sabaté, A., Bureau, S., & Le Bourvellec, C. (2021). Modification of apple, beet and kiwifruit cell walls by boiling in acid conditions: Common and specific responses. *Food Hydrocolloids*, *112*, 106266. https://doi.org/10.1016/j.foodhyd.2020.106266

Liu, X., Renard, C. M. G. C., Rolland-Sabaté, A., & Le Bourvellec, C. (2021). Exploring interactions between pectins and procyanidins: Structure-function relationships. *Food Hydrocolloids*, *113*, 106498. https://doi.org/10.1016/j.foodhyd.2020.106498

Loo, Y. T., Howell, K., Chan, M., Zhang, P., & Ng, K. (2020). Modulation of the human gut microbiota by phenolics and phenolic fiber-rich foods. *Comprehensive Reviews in Food Science and Food Safety*, *19*(4), 1268–1298. https://doi.org/10.1111/1541-4337.12563

Micard, V., Renard, C. M. G. C., & Thibault, J. F. (1994). Studies on Enzymic Release of Ferulic Acid from Sugar-Beet Pulp. *LWT - Food Science and Technology*, *27*(1), 59–66. https://doi.org/10.1006/FSTL.1994.1013

Paudel, E., Boom, R. M., van Haaren, E., Siccama, J., & van der Sman, R. G. M. (2016). Effects of cellular structure and cell wall components on water holding capacity of mushrooms. *Journal of Food Engineering*, *187*, 106–113. https://doi.org/10.1016/j.jfoodeng.2016.04.009

Phan, A. D. T., Williams, B. A., Netzel, G., Mikkelsen, D., D'Arcy, B. R., & Gidley, M. J. (2020). Independent fermentation and metabolism of dietary polyphenols associated with a plant cell wall model. *Food and Function*, *11*(3), 2218–2230. https://doi.org/10.1039/c9fo02987g

Poncet-Legrand, C., Gautier, C., Cheynier, V., & Imberty, A. (2007). Interactions between flavan-3-ols and poly(L-proline) studied by isothermal titration

785 calorimetry: Effect of the tannin structure. *Journal of Agricultural and Food*
786 *Chemistry*, *55*(22), 9235–9240. https://doi.org/10.1021/jf071297o
787 Ralet, M. C., Crépeau, M. J., Vigouroux, J., Tran, J., Berger, A., Sallé, C., … North,
788 H. M. (2016). Xylans provide the structural driving force for mucilage adhesion
789 to the Arabidopsis seed coat. *Plant Physiology*, *171*(1), 165–178.
790 https://doi.org/10.1104/pp.16.00211
791 Renard, C. M. G. C., Baron, A., Guyot, S., & Drilleau, J. F. (2001). Interactions
792 between apple cell walls and native palle polyphenols/quantification and some
793 consequences. *International Journal of Biology Macromolecules*, *29*, 115–125.
794 Renard, C. M. G. C., Voragen, A. G. J., Thibault, J. F., & Pilnik, W. (1990). Studies
795 on apple protopectin: I. Extraction of insoluble pectin by chemical means.
796 *Carbohydrate Polymers*, *12*(1), 9–25.
797 https://doi.org/10.1016/0144-8617(90)90101-W
798 Renard, C. M. G. C., Voragen, A. G. J., Thibault, J. F., & Pilnik, W. (1991). Studies
799 on apple protopectin. IV: Apple xyloglucans and influence of pectin extraction
800 treatments on their solubility. *Carbohydrate Polymers*, *15*(4), 387–403.
801 https://doi.org/10.1016/0144-8617(91)90089-U
802 Renard, C. M. G. C., Watrelot, A. A., & Le Bourvellec, C. (2017). Interactions
803 between polyphenols and polysaccharides: Mechanisms and consequences in
804 food processing and digestion. *Trends in Food Science and Technology*, *60*, 43–
805 51. https://doi.org/10.1016/j.tifs.2016.10.022
806 Ruiz-Garcia, Y., Smith, P. A., & Bindon, K. A. (2014). Selective extraction of
807 polysaccharide affects the adsorption of proanthocyanidin by grape cell walls.
808 *Carbohydrate Polymers*, *114*, 102–114.
809 https://doi.org/10.1016/j.carbpol.2014.07.024
810 Saeman, J. F., Moore, W. E., Mitchell, R. L., & Millett, M. A. (1954). Techniques for
811 the determination of pulp constituents by quantitiative paper chromatography.
812 *Tappi Journal*, *37*(8), 336–343.
813 Santhakumar, A. B., Battino, M., & Alvarez-Suarez, J. M. (2018). Dietary

polyphenols: Structures, bioavailability and protective effects against atherosclerosis. *Food and Chemical Toxicology*, *113*, 49–65. https://doi.org/10.1016/j.fct.2018.01.022

Saura-Calixto, F., & Pérez-Jiménez, J. (2018). *Non-extractable Polyphenols and Carotenoids*. (F. Saura-Calixto & J. Pérez-Jiménez, Eds.) (Vol. 5). Royal Society of Chemistry. https://doi.org/doi.org/10.1039/9781788013208

Tang, H. R., Covington, A. D., & Hancock, R. A. (2003). Structure-Activity Relationships in the Hydrophobic Interactions of Polyphenols with Cellulose and Collagen. *Biopolymers*, *70*(3), 403–413. https://doi.org/10.1002/bip.10499

Tarko, T., & Duda-Chodak, A. (2020). Influence of Food Matrix on the Bioaccessibility of Fruit Polyphenolic Compounds. *Journal of Agricultural and Food Chemistry*, *68*(5), 1315–1325. https://doi.org/10.1021/acs.jafc.9b07680

Tudorache, M., & Bordenave, N. (2019). Phenolic compounds mediate aggregation of water-soluble polysaccharides and change their rheological properties: Effect of different phenolic compounds. *Food Hydrocolloids*, *97*, 1–6. https://doi.org/10.1016/j.foodhyd.2019.105193

Varner, J. E., & Lin, L. S. (1989). Plant cell wall architecture. *Cell*, *56*(2), 231–239. https://doi.org/10.1016/0092-8674(89)90896-9

Velasco, F. G., Luzardo, F. H. M., Guzman, F., Rodriguez, O., Coto Hernandez, I., Barroso, S., & Diaz Rizo, O. (2014). Gamma radiation effects on molecular characteristic of vegetable tannins. *Journal of Radioanalytical and Nuclear Chemistry*, *299*(3), 1787–1792. https://doi.org/10.1007/s10967-014-2921-8

Waldron, K. W., Smith, A. C., Parr, A. J., Ng, A., & Parker, M. L. (1997). New approaches to understanding and controlling cell separation in relation to fruit and vegetable texture. *Trends in Food Science and Technology*, *8*(7), 213–221. https://doi.org/10.1016/S0924-2244(97)01052-2

Waskom, M. (2014). Seaborn: Statistical Data Visualization. Retrieved from http://stanford.edu/~mwaskom/software/seaborn/

Watrelot, A. A., Le Bourvellec, C., Imberty, A., & Renard, C. M. G. C. (2013).

Interactions between pectic compounds and procyanidins are influenced by methylation degree and chain length. *Biomacromolecules*, *14*(3), 709–718. https://doi.org/10.1021/bm301796y

Watrelot, A. A., Le Bourvellec, C., Imberty, A., & Renard, C. M. G. C. (2014). Neutral sugar side chains of pectins limit interactions with procyanidins. *Carbohydrate Polymers*, *99*, 527–536. https://doi.org/10.1016/j.carbpol.2013.08.094

Zykwinska, A. W., Ralet, M.-C. J., Garnier, C. D., & Thibault, J.-F. J. (2005). Evidence for In Vitro Binding of Pectin Side Chains to Cellulose. *Plant Physiology*, *139*(1), 397–407. https://doi.org/10.1104/pp.105.065912

Table 1. Characteristic chemical content, sugar ratios, specific surface area and water binding capacity of the different cell wall components from apple, beet and kiwifruit.

Samples	Gal A/ (Rha+Ara+Gal)	Gal A/Rha	(Ara+Gal)/Rha	Ara/Gal	Xyl/Man	FA* (mg/g)	DM* (%)	Ac.A* (mg/g)	BET (m^2/g)	WBC (g/g)
ACN	1.2	12.4	9.5	1.2	4.9		82	21	5.4	7.8
AC2	1.6	13.0	7.3	0.5	4.9		86	19	1.1	8.5
AC3	0.9	9.1	9.3	1.1	5.1		89	19	1.5	5.9
AC6	0.7	8.9	11.7	1.2	5.0		60	18	2.6	3.9
BCN	0.7	12.3	16.0	4.2	0.7	7.0	65	45	4.5	3.7
BC2	0.9	12.1	12.5	2.4	0.8	7.7	58	41	6.3	7.7
BC3	0.5	8.5	16.3	4.0	0.8	9.6	72	39	2.4	4.2
BC6	0.4	8.9	19.7	4.3	0.8	8.8	42	32	16.7	6.0
KCRN	2.7	28.7	9.5	0.2	2.5		67	11	1.3	5.6
KCR2	2.3	26.5	10.7	0.2	2.6		62	12	0.5	8.0
KCR3	1.5	18.2	11.0	0.3	2.9		70	11	5.9	6.0
KCR6	1.1	15.6	13.4	0.2	2.6		69	11	7.0	6.6
KCON	4.1	38.4	8.4	0.4	2.9		72	11	0.3	4.6
KCO2	2.4	33.4	12.9	0.2	2.6		58	13	1.3	6.9
KCO3	2.2	30.4	13.0	0.3	2.6		65	11	11.4	5.9
KCO6	1.6	18.2	10.4	0.3	2.4		55	11	0.6	4.0
Pooled SD	*0.1*	*1.9*	*0.9*	*0.03*	*0.1*	*0.2*	*4.1*	*0.8*	-	*1.2*

Ratios are calculated using the yields of neutral sugar expressed in mol%. Ratios Gal A/(Rha+Ara+Gal) is characteristic for linearity of pectin. Gal A/Rha for contribution of homogalacturonans to pectin. (Ara+Gal)/Rha for branching of RG-I. Ara/Gal for the proportion of arabinans/galactans. Xyl/Man for contribution of mannans to hemicelluloses. Gal A: galacturonic acid, Rha: rhamnose, Ara: arabinose, Gal: galactose, Man: mannose, Xyl: xylose. DM: degree of methylation. FA and Ac.A: ferulic acid and acetic acid content, respectively. BET and WBC are characteristic for specific surface area and water-binding capacity, respectively. AC: apple cell wall, BC: beet cell wall, KC: kiwifruit cell wall, pH values-: 2: pH 2.0, 3: pH 3.5, 6: pH 6.0. Maturity-: R: −Ripe, O: −Overripe. Pooled SD: pooled standard deviation. * data adapted from (Liu, Renard, Rolland-Sabaté, Bureau, et al., 2021).

Table 2. Binding isotherms between cell walls and procyanidins DP12 and 39: A) Apparent Langmuir parameters for binding isotherms of different cell walls with varying concentrations of procyanidin DP12 and DP39, and B) Procyanidin retention and free procyanidins characteristics at 1 g/L of procyanidins and 5 g/L of cell walls.

A

	Procyanidin DP12					Procyanidin DP39				
	K_L (L/g)	N_{max} (g/g)	K_L (L/m^2)	N_{max} (g/m^2)	R^2	K_L (L/g)	N_{max} (g/g)	K_L (L/m^2)	N_{max} (g/m^2)	R^2
ACN	0.25±0.09	0.75±0.13	0.05±0.02	0.14±0.02	0.91	0.6±0.10	1.18±0.07	0.11±0.02	0.22±0.01	0.96
AC2	0.17±0.03	0.75±0.08	0.15±0.03	0.68±0.07	0.98	0.46±0.09	1.23±0.09	0.42±0.08	1.12±0.08	0.96
AC3	0.16±0.04	0.85±0.12	0.11±0.03	0.57±0.08	0.96	0.36±0.05	1.34±0.07	0.24±0.03	0.89±0.05	0.99
AC6	0.11±0.03	0.76±0.12	0.04±0.01	0.29±0.06	0.97	0.21±0.05	1.56±0.17	0.08±0.02	0.60±0.07	0.97
BCN	0.38±0.06	0.75±0.05	0.08±0.01	0.17±0.01	0.97	0.46±0.10	0.91±0.07	0.10±0.03	0.20±0.02	0.95
BC2	0.33±0.06	0.75±0.05	0.06±0.01	0.12±0.01	0.97	0.37±0.06	1.32±0.09	0.06±0.01	0.21±0.02	0.97
BC3	0.28±0.05	0.65±0.05	0.12±0.02	0.27±0.02	0.97	0.34±0.05	1.09±0.06	0.14±0.03	0.45±0.04	0.98
BC6	0.54±0.05	0.51±0.01	0.03±0.01	0.03±0.01	0.99	0.29±0.05	1.43±0.12	0.02±0.01	0.09±0.01	0.98
KCRN	0.25±0.07	0.49±0.06	0.19±0.05	0.38±0.05	0.93	0.21±0.06	1.73±0.25	0.16±0.05	1.33±0.19	0.95

KCR2	0.17±0.07	0.6±0.13	0.34±0.14	1.20±0.26	0.89	0.13±0.04	2.18±0.42	0.26±0.08	4.36±0.84	0.97
KCR3	0.35±0.05	0.6±0.03	0.06±0.01	0.10±0.01	0.98	0.3±0.08	1.47±0.17	0.05±0.02	0.25±0.03	0.95
KCR6	0.25±0.14	0.58±0.13	0.04±0.02	0.08±0.02	0.89	0.23±0.06	1.15±0.12	0.03±0.01	0.16±0.02	0.96
KCON	0.21±0.05	0.49±0.05	0.70±0.17	1.63±0.17	0.96	0.19±0.05	1.17±0.14	0.63±0.17	3.90±0.47	0.97
KCO2	0.29±0.12	0.37±0.06	0.22±0.09	0.28±0.04	0.85	0.15±0.03	1.36±0.17	0.12±0.02	1.05±0.13	0.98
KCO3	0.24±0.09	0.44±0.07	0.02±0.01	0.04±0.01	0.89	0.41±0.06	0.85±0.05	0.04±0.01	0.07±0.01	0.98
KCO6	0.45±0.09	0.29±0.02	0.75±0.15	0.48±0.03	0.95	0.34±0.08	1.11±0.07	0.57±0.12	1.88±0.2	0.95

B

	Procyanidin DP12			Procyanidin DP39		
	Bound procyanidins (g/g CW)	% of initial PCA	$\overline{DP}n$ of Free PCA	Bound procyanidins (g/g CW)	% of initial PCA	$\overline{DP}n$ of Free PCA
ACN	0.083	44%	3.7	0.148	61%	15.7
AC2	0.078	40%	4.5	0.120	70%	20.8
AC3	0.075	36%	4.4	0.113	59%	15.1
AC6	0.061	32%	4.5	0.104	55%	16.4
BCN	0.085	51%	3.8	0.116	59%	20.7
BC2	0.086	45%	3.8	0.110	55%	16.4

BC3	0.067	42%	4.2	0.111	55%	12.4
BC6	0.091	53%	4.2	0.108	54%	15.7
KCRN	0.071	38%	4.4	0.091	47%	19.7
KCR2	0.069	37%	4.1	0.084	46%	16.7
KCR3	0.083	41%	4.3	0.100	57%	21.9
KCR6	0.077	41%	4.4	0.112	64%	21.5
KCON	0.063	35%	4.5	0.104	57%	20.8
KCO2	0.077	42%	4.3	0.104	48%	14.1
KCO3	0.090	47%	4.2	0.126	69%	14.4
KCO6	0.071	40%	4.3	0.114	61%	18.5
Pooled SD	*0.002*	*0.01*	*0.2*	*0.003*	*0.02*	*1.0*

Average of duplicates for each; uncertainty on the parameters of the Langmuir isotherms in Table 2A was calculated using the Marquardt estimation approach, precision on the analytical results in Table 2B using pooled standard deviation.. $\overline{DP}n$: number-average degree of polymerization of procyanidins, K_L: apparent affinity constant, N_{max}: apparent saturation level. AC: apple cell wall, BC: beet cell wall, KC: kiwifruit cell wall, pH values-: 2: pH 2.0, 3: pH 3.5, 6: pH 6.0. Maturity-: R: −Ripe, O: −Overripe. Pooled SD: pooled standard deviation.

Table 3. Thermodynamic parameters of interactions between cell walls and procyanidins DP12 and DP39 (30 mM (-)-epicatechin equivalent) measured by Isothermal Titration Microcalorimetry (ITC).

		Procyanidin DP12					Procyanidin DP39				
	n	K_a (M^{-1})	ΔH (kJ/mol)	ΔS (J/mol/K)	ΔG (kJ/mol)	-TΔS (kJ/mol)	K_a (M^{-1})	ΔH (kJ/mol)	ΔS (J/mol/K)	ΔG (kJ/mol)	-TΔS (kJ/mol)
ACN	0.1	3180	-1.38	62.44	-19.99	-18.62	1087	-4.36	43.50	-17.33	-12.97
AC2	0.1	1056	-7.42	33.01	-17.26	-9.84	752	-8.13	27.79	-16.42	-8.29
AC3	0.1	375	-11.96	9.16	-14.69	-2.73	932	-8.20	29.33	-16.95	-8.75
AC6	0.1	1166	-7.05	35.05	-17.51	-10.45	275	-15.19	-4.24	-13.92	1.27
BCN	0.1	179	-14.20	-4.50	-12.86	1.34	251	-12.34	4.57	-13.70	-1.36
BC2	0.1	395	-11.00	12.81	-14.82	-3.82	191	-16.19	-10.64	-13.02	3.17
BC3	0.1	208	-22.17	-29.98	-13.23	8.94	119	-33.72	-73.35	-11.85	21.87
BC6	0.1	1690	-6.25	40.85	-18.43	-12.18	212	-22.01	-29.28	-13.28	8.73
KCRN	0.1	2848	-7.46	41.11	-19.72	-12.26	451	-18.39	-15.29	-15.15	3.24
KCR2	0.1	693	-22.09	-19.71	-16.22	5.87	717	-18.52	-7.45	-16.30	2.22
KCR3	0.1	840	-32.74	-53.81	-16.69	16.05	444	-26.48	-38.12	-15.11	11.37
KCR6	0.1	951	-46.09	-97.56	-17.00	29.09	1334	-12.61	17.53	-17.84	-5.23
KCON	0.1	2273	-8.49	35.80	-19.16	-10.68	526	-12.75	9.33	-15.53	-2.78
KCO2	0.1	895	-19.41	-8.59	-16.85	2.56	1589	-4.07	47.60	-18.27	-14.21
KCO3	0.1	1188	-28.99	-38.37	-17.55	11.44	562	-22.73	-23.61	-15.69	7.04
KCO6	0.1	2180	-0.82	61.18	-19.06	-18.24	1527	-6.62	38.73	-18.17	-11.55
Pooled SD	-	*256*	*1.1*	*2.1*	*0.3*	*0.6*	*104*	*0.8*	*2.1*	*0.2*	*0.6*

Average of duplicates for each. $\overline{DP}n$: number-average degree of polymerization of procyanidins, K_a: affinity level, n: stoichiometry, ΔH: enthalpy, ΔG: free enthalpy, ΔS: entropy. AC: apple cell wall, BC: beet cell wall, KC: kiwifruit cell wall, pH values-: 2: pH 2.0, 3: pH 3.5, 6: pH 6.0. Maturity-: R: −Ripe, O: −Overripe.

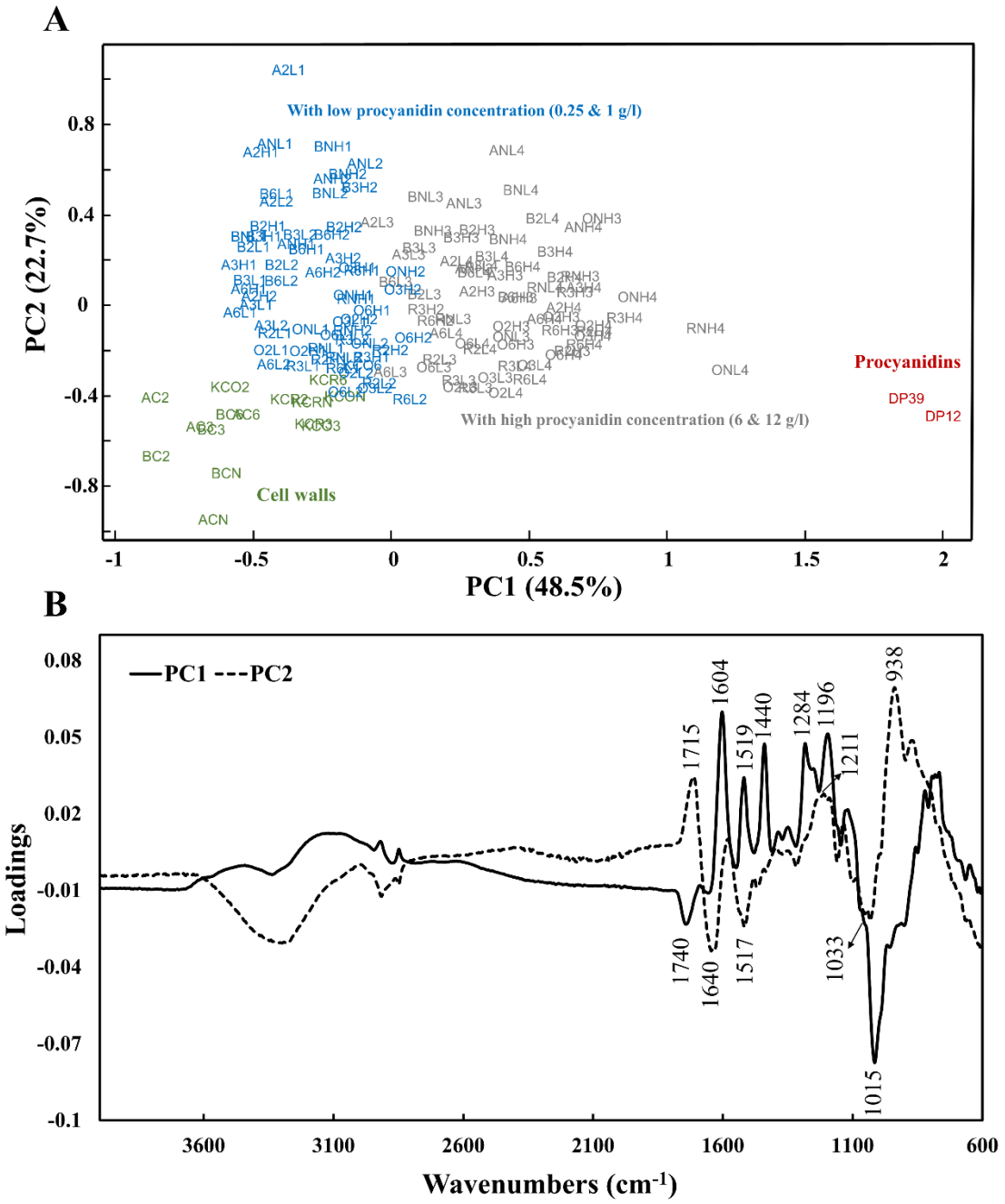

Fig. 1. Principal component analysis of infrared spectra on cell walls, procyanidins and their complexes. A) Sample map; B) Loading profile of components PC1 and PC2 in the range of 4000 - 600 cm^{-1}. A(C): apple cell wall, B(C): beet cell wall, (KC)R: kiwifruit cell wall (ripe), (KC)O: kiwifruit cell wall (overripe), L/H1: 0.25 g/l DP12/39, L/H2: 1 g/l DP12/39, L/H3: 6 g/l DP12/39, L/H4: 12 g/l DP12/39, N: native, pH values-: 2: pH 2.0, 3: pH 3.5, 6: pH 6.0. Maturity-: R: −Ripe, O: −Overripe.

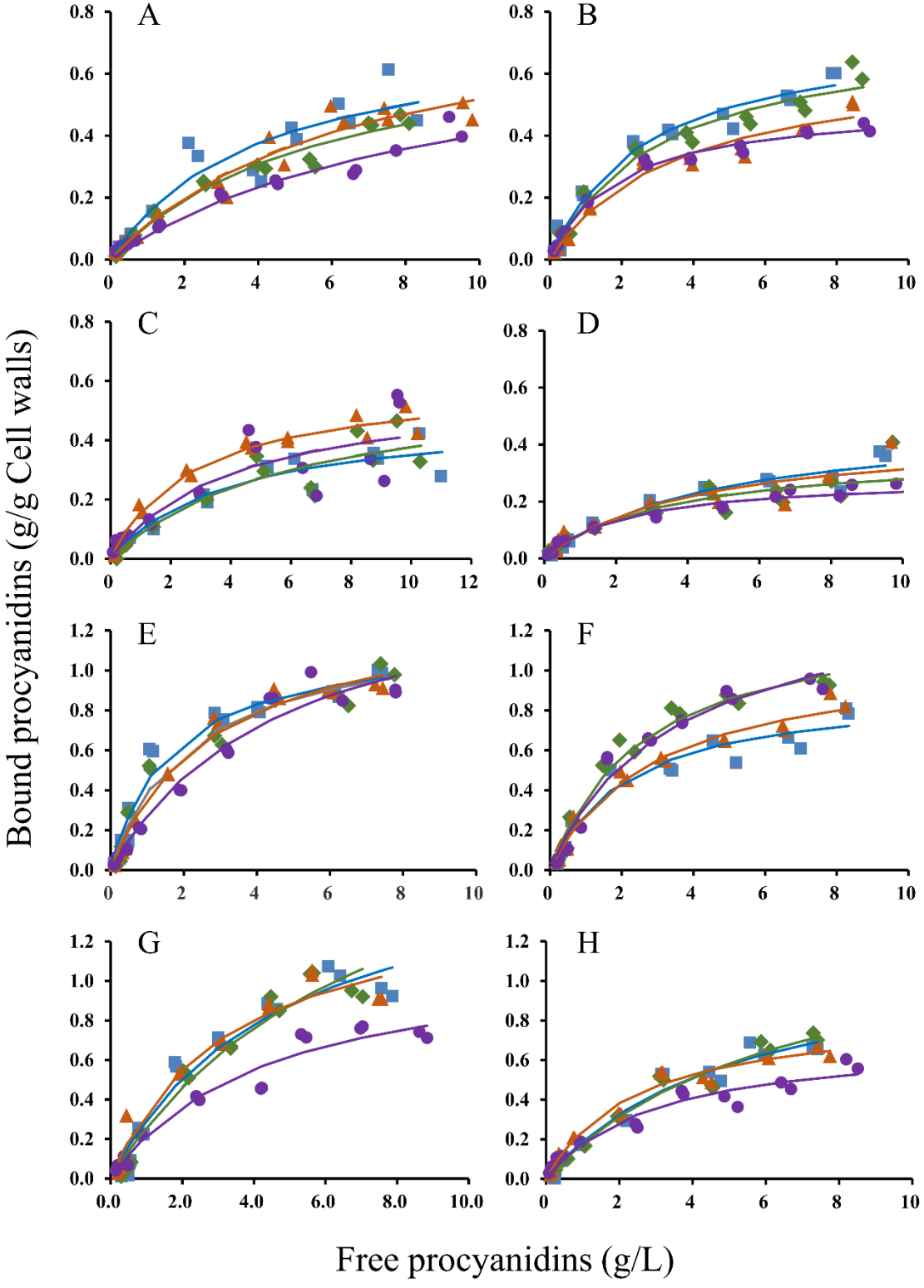

877

878 **Fig. 2.** Binding isotherms for cell walls and procyanidins at pH 3.8, ionic strength 0.1 mol/L, 25 °C. A:
879 experimental curve for ACs-DP12 complexes, B: experimental curve for BCs-DP12 complexes, C: experimental
880 curve for KCRs-DP12 complexes, D: experimental curve for KCOs-DP12 complexes, E: experimental curve for
881 ACs-DP39 complexes, F: experimental curve for BCs-DP39 complexes, G: experimental curve for KCRs-DP39
882 complexes, H: experimental curve for KCOs-DP39 complexes. The points and lines are the corresponding
883 Langmuir adsorption isotherms for which the calculated parameters are given in Table 2 for different cell walls: ■

and — Native cell walls, ◆ and — Cell walls modified at pH 2.0, ▲ and — Cell walls modified at pH 3.5, ● and — Cell walls modified at pH 6.0.

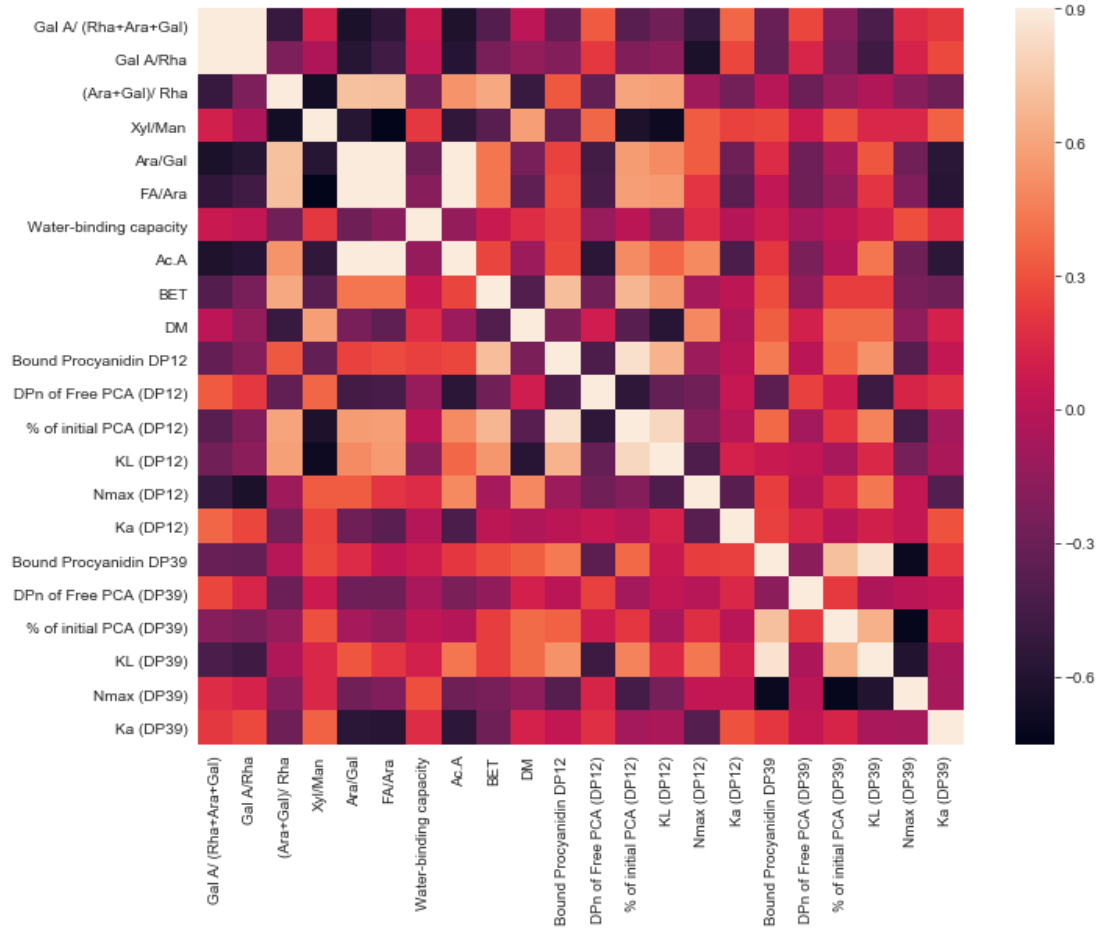

Figure 3. Correlation matrix heatmap between carbohydrate compositions and structural characteristics of cell walls and binding properties after interaction with procyanidins. Ratios Gal A/(Rha+Ara+Gal) is characteristic for linearity of pectin. Gal A/Rha for contribution of homogalacturonans to pectin. (Ara+Gal)/Rha for branching of RG-I. Ara/Gal for the proportion of arabinans/galactans. Xyl/Man for contribution of mannans to hemicelluloses. DM: degree of methylation. FA and Ac.A: ferulic acid and acetic acid content, respectively. BET and WBC are characteristic for specific surface area and water-binding capacity, respectively.